NeuroImage: Clinical 16 (2017) 595–603

Contents lists available at ScienceDirect

NeuroImage: Clinical

journal homepage: www.elsevier.com/locate/ynicl

Longitudinal white matter change in frontotemporal dementia subtypes and sporadic late onset Alzheimer's disease

Fanny M. Elahi[a,*], Gabe Marx[a], Yann Cobigo[a], Adam M. Staffaroni[a], John Kornak[b], Duygu Tosun[c,d], Adam L. Boxer[a], Joel H. Kramer[a], Bruce L. Miller[a], Howard J. Rosen[a,*]

[a] Memory and Aging Center, Department of Neurology, University of California, San Francisco, United States
[b] Department of Epidemiology and Biostatistics, University of California, San Francisco, United States
[c] Department of Veteran Affairs Medical Center, San Francisco, CA, United States
[d] Department of Radiology and Biomedical Imaging, University of California, San Francisco, United States

ARTICLE INFO

Keywords:
Longitudinal
DTI
White matter integrity
Sample size
Clinical trial
FTD
AD
Behavioral variant FTD
Primary progressive aphasia

ABSTRACT

Background: Degradation of white matter microstructure has been demonstrated in frontotemporal lobar degeneration (FTLD) and Alzheimer's disease (AD). In preparation for clinical trials, ongoing studies are investigating the utility of longitudinal brain imaging for quantification of disease progression. To date only one study has examined sample size calculations based on longitudinal changes in white matter integrity in FTLD.
Objective: To quantify longitudinal changes in white matter microstructural integrity in the three canonical subtypes of frontotemporal dementia (FTD) and AD using diffusion tensor imaging (DTI).
Methods: 60 patients with clinical diagnoses of FTD, including 27 with behavioral variant frontotemporal dementia (bvFTD), 14 with non-fluent variant primary progressive aphasia (nfvPPA), and 19 with semantic variant PPA (svPPA), as well as 19 patients with AD and 69 healthy controls were studied. We used a voxel-wise approach to calculate annual rate of change in fractional anisotropy (FA) and mean diffusivity (MD) in each group using two time points approximately one year apart. Mean rates of change in FA and MD in 48 atlas-based regions-of-interest, as well as global measures of cognitive function were used to calculate sample sizes for clinical trials (80% power, alpha of 5%).
Results: All FTD groups showed statistically significant baseline and longitudinal white matter degeneration, with predominant involvement of frontal tracts in the bvFTD group, frontal and temporal tracts in the PPA groups and posterior tracts in the AD group. Longitudinal change in MD yielded a larger number of regions with sample sizes below 100 participants per therapeutic arm in comparison with FA. SvPPA had the smallest sample size based on change in MD in the fornix (n = 41 participants per study arm to detect a 40% effect of drug), and nfvPPA and AD had their smallest sample sizes based on rate of change in MD within the left superior longitudinal fasciculus (n = 49 for nfvPPA, and n = 23 for AD). BvFTD generally showed the largest sample size estimates (minimum n = 140 based on MD in the corpus callosum). The corpus callosum appeared to be the best region for a potential study that would include all FTD subtypes. Change in global measure of functional status (CDR box score) yielded the smallest sample size for bvFTD (n = 71), but clinical measures were inferior to white matter change for the other groups.
Conclusions: All three of the canonical subtypes of FTD are associated with significant change in white matter integrity over one year. These changes are consistent enough that drug effects in future clinical trials could be detected with relatively small numbers of participants. While there are some differences in regions of change across groups, the genu of the corpus callosum is a region that could be used to track progression in studies that include all subtypes.

1. Introduction

FTLD is a pathological term used to designate a group of neurodegenerative disorders that primarily affect the frontal and temporal lobes (Brun, 1987; Gorno-Tempini et al., 2011). FTLD is associated with a variety of clinical presentations, including three of the

* Corresponding authors at: Department of Neurology, Memory and Aging Center, University of California, San Francisco, 675 Nelson Rising Lane, San Francisco, CA 94158, United States.
E-mail addresses: fanny.elahi@ucsf.edu (F.M. Elahi), howie.rosen@ucsf.edu (H.J. Rosen).

http://dx.doi.org/10.1016/j.nicl.2017.09.007
Received 14 March 2017; Received in revised form 17 August 2017; Accepted 6 September 2017
Available online 14 September 2017
2213-1582/ © 2017 The Authors. Published by Elsevier Inc. This is an open access article under the CC BY-NC-ND license (http://creativecommons.org/licenses/BY-NC-ND/4.0/).

most commonly described subtypes of FTD: bvFTD, nfvPPA, and svPPA (Johnson et al., 2005; Galantucci et al., 2011). These three syndromes differ in their clinical features, with bvFTD presenting primarily with changes in socioemotional function (Gorno-Tempini et al., 2011; Seeley, 2008; Garcin et al., 2009), svPPA with loss of knowledge about words, and objects, and nfvPPA with agrammatism, nonfluent speech and articulatory difficulties (Wilson et al., 2009; Wilson et al., 2010). Yet the three syndromes are linked by a relatively limited number of underlying proteinopathies. The two most common molecular pathologies include abnormal depositions of Tau or TDP-43 (TAR DNA-binding protein 43) (Neumann et al., 2006; Baborie et al., 2011). In some cases, the clinical syndrome strongly predicts the underlying pathology, as is the case with svPPA, which is associated with TDP-43 type C in about 83% of cases (Spinelli et al., 2017), or autosomal dominant genetic cases of bvFTD, such as *GRN* or *C9orf72* mutations, also associated with TDP-43 pathology. However, for the most part, clinico-pathological correlations continue to pose important diagnostic challenges. For instance, nfvPPA is often associated with tauopathy, although in certain cohorts a high frequency of TDP-43 pathology is reported [11,] (Boxer et al., 2006). The bvFTD clinical syndrome remains the most pathologically heterogenous subtype, caused most frequently by TDP-43 and tau pathologies, less frequently FUS, in addition to other more rare pathologies (Spinelli et al., 2017; Mann and Snowden, 2017; Munoz et al., 2009; Grossman, 2010).

As it stands, there are no approved therapies for FTLD, however efforts to develop treatments are ongoing (Zhang et al., 2016; Rojas and Boxer, 2016). In preparation for future clinical trials, efficient measures of disease progression that allow detection of drug effects with the smallest possible number of participants need to be developed. The heterogeneity in clinical presentations of FTLD proteinopathies makes this problem particularly complex. Future therapeutic trials will target specific proteinopathies. Therefore, once a biomarker is available to identify the proteinopathy for each case of FTLD *in vivo*, the ability to enroll any patient with the targeted protein disorder, irrespective of the specificity of their symptoms, would increase power. Drugs targeting tau, for instance, may include bvFTD and nfvPPA patients. In such trials, it would be difficult to choose an appropriate specific symptom-related outcome measure. Whereas language tasks may be appropriate for nfvPPA or svPPA, they would likely be insensitive to change in bvFTD within the optimal therapeutic window. Thus, in addition to global cognitive measures and assessment of functional abilities, there would be value in identifying quantifiable intermediate phenotypes, standing between the underlying molecular pathologies and clinical phenotypes. Such measures would be anticipated to be equally applicable to a variety of clinical syndromes, as well as perhaps especially needed for the study of specific subgroups, such as bvFTD patients with a slowly progressive, subcortical form of neurodegeneration (Ranasinghe et al., 2016).

Diffusion tensor imaging, which utilizes measures of water diffusion to assess microstructural alterations in white matter, has been used in cross-sectional and longitudinal assessment of white matter degeneration in FTD (Galantucci et al., 2011; Zhang et al., 2016; Acosta-Cabronero et al., 2011; Agosta et al., 2014; Borroni et al., 2007; Mahoney et al., 2015; Matsuo et al., 2008; Schwindt et al., 2013; Whitwell et al., 2010; Zhang et al., 2009; Lam et al., 2014; Floeter et al., 2016; Tu et al., 2016). This is consistent with pathological studies demonstrating that, in addition to neuronal cell death, FTLD brains also show substantial gliosis and degeneration of white matter tracts (Lant et al., 2014). Moreover, recent studies showed that longitudinal white matter changes over a 12 month period are more extensive than grey matter (Whitwell et al., 2010). Studies in bvFTD have demonstrated favorable effect sizes for white matter changes when compared to clinical or volumetric grey matter changes (Mahoney et al., 2015; Santillo et al., 2013). This suggests that longitudinal measures of white matter integrity may be excellent markers of pathological progression in FTLD.

The goal of this study was to quantify longitudinal changes in white matter integrity using DTI in bvFTD, svPPA and nfvPPA and to assess the utility of DTI as a metric of disease progression in each of these variants. In order to evaluate the specificity of the findings, we also examined longitudinal white matter changes in AD, a neurodegenerative disease affecting posterior rather than frontotemporal brain regions, with proteinopathies that differ from those noted in FTLD.

2. Methods

2.1. Participants

A total of 148 participants were included in this retrospective study. The study participants were individuals enrolled in ongoing longitudinal studies at the Memory and Aging Center at UCSF (MAC) who had undergone MRI twice approximately one year apart and were given the following diagnoses: bvFTD (n = 27), nfvPPA (n = 14), svPPA (n = 19), and AD (n = 19). Our control group was composed of participants who also had MRI scans approximately one year apart and were not given a diagnosis of neurodegenerative disease, and considered neurologically and cognitively normal (n = 69). Patients included in this study were recruited between 2008 and 2016 through ongoing studies (AG019724, AG032306, AG023501) at the MAC. Diagnoses were based on a multidisciplinary evaluation including neurological exam and symptomatic evaluation, neuropsychological and nursing evaluations, and socioemotional assessments. Disease duration was estimated based on the year of initial symptoms provided by the patient or their informant. All study participants were provided informed consent and the study protocols were approved by the UCSF Committee on Human Research. Research was performed in accordance with the Code of Ethics of the World Medical Association.

2.2. MRI acquisition

MR images were acquired on a 3 Tesla Siemens Tim Trio system equipped with a 12-channel head coil at the UCSF Neuroscience Imaging Center. Diffusion sequences were acquired using the following parameters: TR/TE 8200/86 ms; B = 0 image and 64 directions at B = 2000 s/mm^2; FOV 220 × 220 mm^2 and 2.2 mm thick slices; matrix 100 × 100 with 60 slices yielding 2.2 mm^3 isotropic voxels/(TR/TE 8000/109 ms; B = 0 image and 64 directions at B = 2000 s/mm^2; FOV 220 × 220 mm^2 and 2.2 mm thick slices; matrix 100 × 100 with 55 slices yielding 2.2 mm^3 isotropic voxels).

2.3. DTI processing

Processing of diffusion images was carried out using the FSL and Dipy utilities. The b = 0 image was co-registered to the diffusion direction images to create one 4D image followed by gradient direction eddy current and distortion correction. Diffusion tensors were calculated using a non-linear least-squares algorithm. To ensure our measurements were restricted to white matter tissue and not biased by atrophy, all data (both cross-sectional and longitudinal, ROI and voxel-based) was sampled from voxels which had a minimum FA value of 0.1 across all subjects.

2.4. Longitudinal registration

Longitudinal registration of diffusion data was accomplished through the DTI-TK software package (http://dti-tk.sourceforge.net) based on previously published methods: (http://www.sciencedirect.com/science/article/pii/S1053811913000918) (Keihaninejad et al., 2013). DTI-TK implements a tensor-based registration paradigm, maximizing the alignment of white matter structures and minimizing interpolation of DTI images. Intra-subject templates were created through iterative non-linear and linear registration of baseline and follow-up

Table 1
Summary of demographic and basic clinical data for all groups.

Diagnosis	Controls n = 69		bvFTD n = 27		nfvPPA n = 14		svPPA n = 19		AD n = 19		ANOVA n = 148
	Mean	SD	Mean	SD	Mean	SD	Mean	SD	Mean	SD	
Smx onset (age)	N/A	N/A	53.56	7.54	63.14	5.39	57.11	8.91	55.79	9.20	p = 0.0058*
Disease duration, baseline, yr	N/A	N/A	5.87	4.11	4.86	3.46	5.84	3.01	5.00	2.37	p = 0.6987
Age at baseline scan, yr	64.19	6.70	59.43	6.84	68.00	7.18	62.95	7.12	60.79	9.01	p = 0.0025*
Follow-up scan (age)	65.36	7.03	60.38	6.80	68.95	7.30	63.90	7.10	62.09	8.92	p = 0.0031*
Interscan interval, yr	1.17	0.60	0.95	0.22	0.95	0.35	0.95	0.37	1.30	0.47	p = 0.0387*
Sex, M/F, #	1.52	0.50	1.41	0.50	1.43	0.51	1.58	0.51	1.53	0.51	p = 0.7671
Education, yr	17.59	1.94	15.78	2.95	16.46	2.79	16.50	2.71	16.83	3.22	p = 0.0262*
MMSE baseline	29.52	0.68	24.81	3.62	23.64	8.44	22.42	7.86	21.94	6.16	p < 0.00001*
MMSE follow-up	27.98	7.29	19.78	9.94	18.08	12.23	18.89	6.98	14.26	10.96	p < 0.00001*
CDRTot baseline	0.00	0.00	6.80	2.80	2.40	2.60	4.10	1.80	5.30	0.40	p < 0.0001*
CDRBox baseline	0.00	0.00	1.20	0.60	0.50	0.50	0.70	0.40	0.90	2.00	p < 0.0001*
CDRTot follow-up	0.00	0.00	8.50	3.00	3.40	3.80	5.50	2.70	5.60	3.90	p < 0.0001*
CDRBox follow-up	0.00	0.00	1.50	0.60	0.70	0.60	1.00	0.50	0.70	1.50	p < 0.0001*

bvFTD, behavioral variant frontotemporal dementia; nvfPPA, non-fluent/agrammatic primary progressive aphasia; svPPA, semantic variant primary progressive aphasia, AD, Alzheimer's disease; ANOVA, analysis of variance; Smx, symptom; yr, years; M, male; F, female; MMSE, Mini-Mental State Examination score; CDRTot, clinical dementia rating score total; CDRBox, CDR box score.

* Significant differences $p < 0.05$.

diffusion tensor images. A similar process was repeated at the intra-subject level using the intra-subject templates to create a groupwise template. Deformations from native space to intra-subject space and from individual subject to group space were concatenated and applied to individual time point images, bringing them to groupwise space. Once in groupwise space, diffusion tensor images were diagonalized into eigenvectors from which fractional anisotropy and mean diffusivity maps were calculated. Regions of interest were extracted from the ICVM-DTI-81 white matter labels and tract atlas (Mori, S., Wakana, S., Nagae-Poetscher, L., van Zijl, P., 2005. MRI atlas of Human White Matter. Elsevier B. V).

2.5. Voxel-based analyses

2.5.1. Cross sectional

Cross-sectional voxel-based maps were prepared using tract-based spatial statistics (TBSS v 1.1; Smith et al., 2006), part of the Functional MRI of the Brain Software Library (FSL v 4.1.9; Smith et al., 2004). Because the diffusion data was already in groupwise space through DTI-TK, we only utilized the TBSS skeletonization technique to ensure inter-subject alignment of tract peaks.

2.5.2. Longitudinal

Longitudinal change maps were created by an initial smoothing of the time-point images with a 4 mm FWHM kernel. Once smoothed, follow-up images were subtracted from baseline images and the difference was divided by the inter-scan-interval in units of years. The annualized change maps were then subsequently smoothed with another 4 mm FWHM kernel.

2.6. Voxel-based statistics

In both cross-sectional and longitudinal paradigms, voxel-based statistics were performed using FSL Randomize (Winkler AM, Ridgway GR, Webster MA, Smith SM, Nichols TE. Permutation inference for the general linear model. NeuroImage, 2014;92:381–397). A voxel-wise general linear model was applied and multiple comparison corrections was performed using a permutation-based (5000 permutations) threshold with threshold-free cluster enhancement.

2.7. Statistical analysis and sample size calculations

Estimation of sample sizes was based on the mean rate of change and standard deviation in each group in atlas-based regions of interest for each DTI metric. Hypothetical drug effect was set at 25% (Supplemental data) and 40% reduction in yearly change, with 80% power, and alpha of 5%.

3. Results

3.1. Demographics, and basic clinical data

Demographic and global cognitive and functional scores of study participants are presented in Table 1. Groups were well matched for age, sex, years of education, and disease duration. As expected and in agreement with previously reported differences in mean age of symptomatic onset among clinical syndromes, significant group differences were observed for age at first symptom and evaluation, as well as measures of global cognition and functional state.

3.2. Cross-sectional voxel-wise white matter assessment across groups

In order to identify regions of significant abnormality at baseline in each group, baseline FA and MD maps in disease groups were compared to the control group.

Whole-brain voxel-wise analyses showed significant differences in measures of white matter integrity between groups at baseline for FA and MD (Fig. 1, green colored voxels). All groups showed significantly lower FA and higher MD values in comparison to controls ($p < 0.05$, corrected), with a different distribution of affected voxels in each group. As expected, the three FTD subtypes had lower FA and higher MD values in tracts connecting to the frontal and temporal lobes, whereas AD patients showed preferential white matter degradation in posterior cerebral regions.

There were no regions where the control group showed significantly more abnormal white matter in comparison to patient groups.

3.3. Longitudinal white matter assessment across groups

Annual rate of change was significantly different in all disease groups compared with controls, with a larger number of significantly affected voxels for MD in comparison with FA (Fig. 1, red-yellow voxels).

For all groups, longitudinal change in white matter occurred mostly in areas of baseline abnormality. The svPPA and nfvPPA groups showed larger numbers of voxels with statistically significant change in

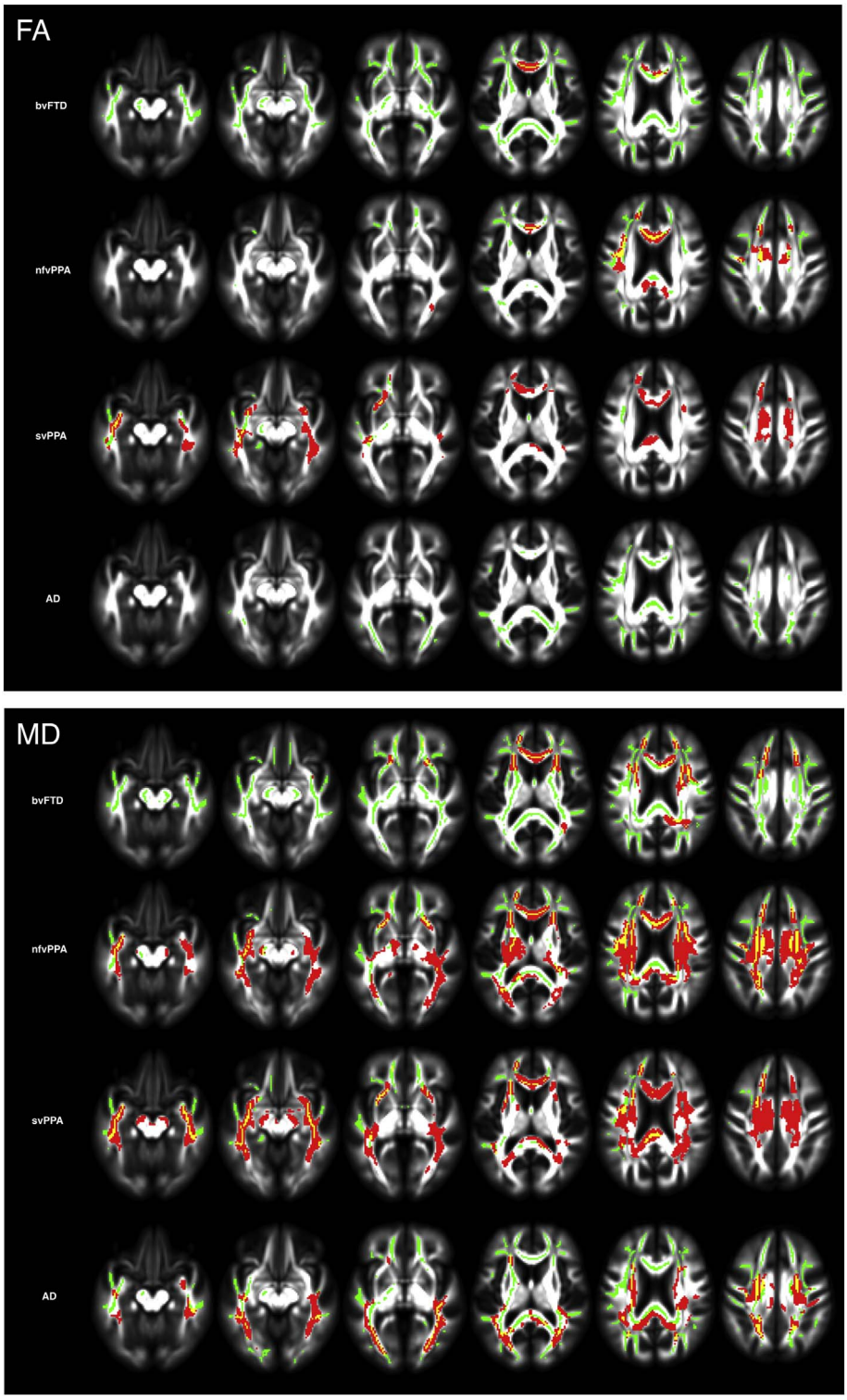

Fig. 1. Cross-sectional and longitudinal white matter changes in bvFTD, nfvPPA, svPPA, and AD. Longitudinal voxel-wise group changes (red) superimposed on baseline skeletonized voxel-wise group differences in comparison with the control group (green). 1.A shows results for FA and 1.B for MD. Results are overlaid on axial sections of the MNI standard brain ($p < 0.05$, corrected for multiple comparisons).

comparison with bvFTD. The PPA groups showed change in bilateral frontotemporal white matter, with a slight left-sided predominance. Although bvFTD showed reduced integrity compared with controls in much of the white matter at baseline, longitudinal change in this group reached statistical significance mostly in the frontal white matter, a more restricted pattern in comparison with the PPA groups. While the FTD groups showed more extensive white matter change in frontotemporal regions, in AD mostly posterior white matter showed significant change over one year.

3.4. Sample size calculations

The results for voxel-wise sample sizes are displayed in Fig. 2, which shows maps of voxel groups yielding sample sizes between 50 and 400 participants per study arm. As expected, frontotemporal regions, with a slight left-predominance produced the smallest sample sizes for PPA groups, whereas the smallest sample sizes were found predominantly in frontal white matter for the bvFTD group. Additionally, consistent with the posterior predominance of white matter change in AD, the smallest sample sizes were within posterior cerebral regions in this group.

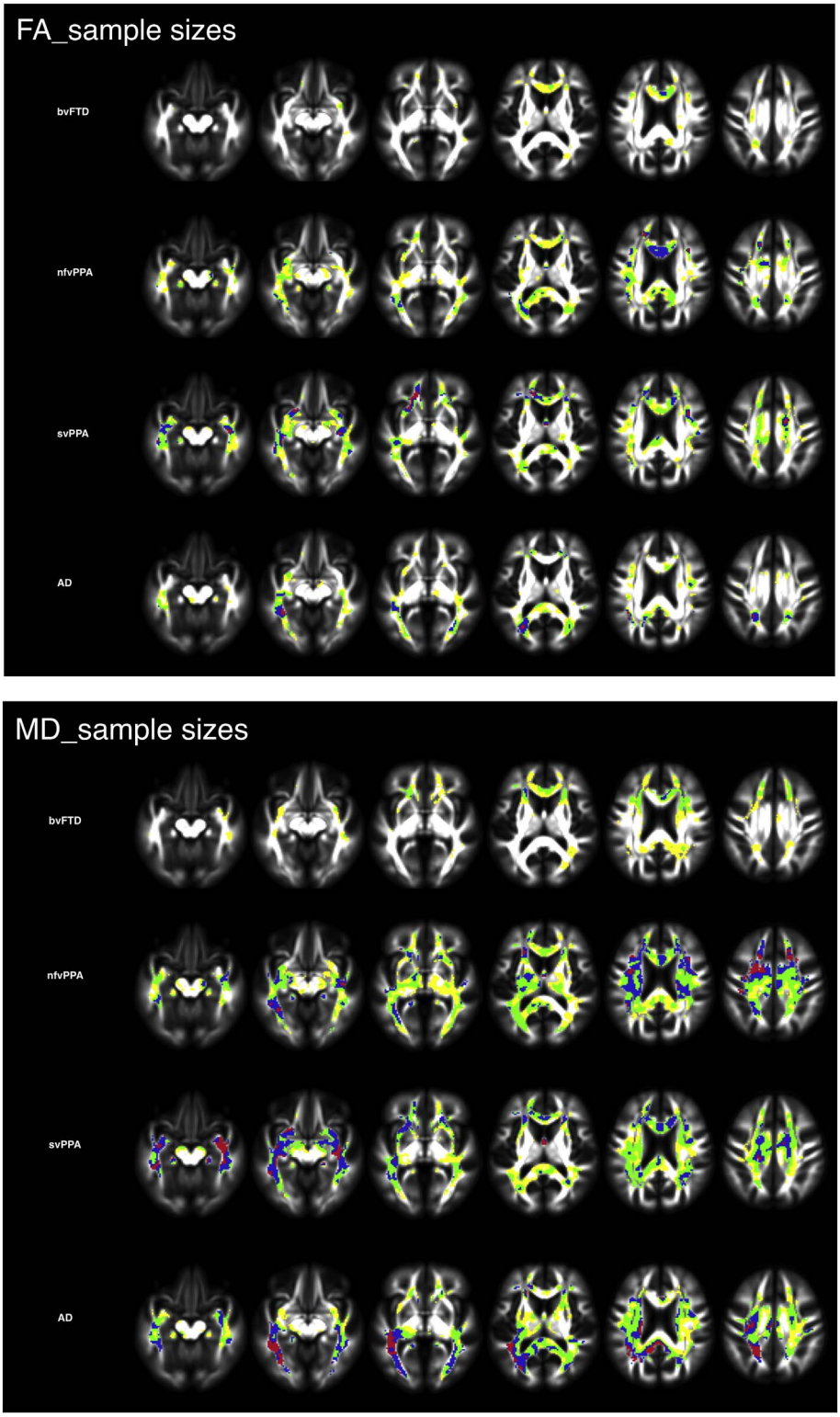

Fig. 2. Voxel-wise sample size calculations for bvFTD, nfvPPA, svPPA, and AD. Red < 50; blue = 50–100, yellow = 100–200, green = 200–400. Sample sizes based on change in FA (2A) and MD (2B).

Although smaller sample sizes were calculated based on voxel-wise change in MD in all groups, especially in the AD group, change in FA and MD showed a high degree of overlap (Fig. 2).

For ROI-based sample size calculations, we report on all regions yielding a sample size estimate of < 100 participants per study arm, in at least one disease group (Table 2.A), and include tables with all samples size values across all 48 tracts investigated as Supplemental data. Using mean annual rate of change in FA, the svPPA group showed the largest number of regions with sample size below 100, followed by nfvPPA (Table 2.A). The smallest sample size for svPPA and bvFTD were in the genu of the corpus callosum (n = 78 for svPPA; n = 162 for bvFTD). Whereas, the smallest sample size for nfvPPA was in the left tapetum (n = 72), and the smallest sample size for the AD group in the left sagittal stratum (n = 91). More regions were found with small sample sizes based on MD measures. Using change in MD, the smallest sample sizes in FTD groups were in the fornix for svPPA (n = 41), the genu of the corpus callosum for bvFTD (n = 140), and for nfvPPA and AD, the left anterior limb of the internal capsule yielded the smallest

Table 2
Illustrated in these tables are sample sizes based on annualized rates of change in FA (2.A) and MD (2.B) in select regions of interest where at least one group had a sample size below 100. A total of 48 regions were investigated. Values under 100 are highlighted in yellow for nfvPPA, purple for svPPA, and blue for AD. Sample sizes are in an ascending order and grouped by pathology. The best sample size for each group is bolded. The region with the overall best sample size, all FTD groups included is the corpus callosum, bordered in red.

FA, fractional anisotropy; MD, mean diffusivity; ROI, region of interest; CC, corpus callosum; fasc., fascicule; Sup, superior; Ant, anterior; L, left; R, right; bvFTD, behavioral variant frontotemporal dementia; nfvPPA, non-fluent/agrammatic primary progressive aphasia; svPPA, semantic variant primary progressive aphasia, AD, Alzheimer's disease.

TABLE II.A. FA ROI-based Sample Sizes

Based on FA values

Group/ROI	Tapetum L	Splenium of CC	Genu of CC	Body of CC	Ant corona radiata R	Sagittal stratum L
Control	1220	4150	2269	1286	1318	6282
bvFTD	8297	946	**162**	50683	465	4287
nfvPPA	**72**	79	124	103	2233	184
svPPA	85	192	**78**	79	80	89
AD	102	193	1015	2144	787	**91**

TABLE II.B. MD ROI-based Sample Sizes

Group/ROI	Ant limb of IC L	SLF R	Sup fronto-occipital fasci L	Genu of CC	Post limb IC L	Tapetum L
Control	3733	3170	35077	2041	1458	856
bvFTD	306	445	488	**140**	11196	1154
nfvPPA	**62**	**62**	80	97	93	99
svPPA	525	138	191	138	1450	132
AD	611	120	195	115	249	161

Group/ROI	Fornix	Uncinate fasciculus R	Sagittal stratum L	Ant corona radiata R	Sagittal stratum R	Stria terminalis L	Body of CC	External capsule L
Control	1999	15805	927	555	10090	924	2856	1928
bvFTD	3879	223	557	153	1801	5518	277637	680
nfvPPA	165	70226	116	101	183	94	115	108
svPPA	**41**	44	52	82	83	85	89	90
AD	1566	280	89	193	140	188	4244	158

Group/ROI	SLF L	Cingulum (gyrus) L	Cingulum (gyrus) R	Post thalamic radiation L	Splenium of CC	Sup corona radiata L	Post corona radiata L	Retrolenticular IC L	Ant corona radiata L
Control	1790	2264	5378	1153	2010	2376	1661	783	3333
bvFTD	581	329	986	3800	456	688	958	13670	169
nfvPPA	**49**	91	490	96	91	71	109	207	125
svPPA	139	155	109	153	128	143	149	800	155
AD	**23**	32	37	51	57	58	67	81	98

sample size (n = 49 for nfvPPA, and n = 23 for AD).

The genu of the corpus callosum emerges as the region with the most consistent change in white matter across all FTD groups, and consequently the smallest sample sizes, taking all FTD subtypes into consideration. This was true for both FA and MD.

Calculations based on annual rate of change in clinical measures, such as quantitative assessment of functional status with clinical dementia rating score (CDR), and global measure of cognition with the mini-mental status examination (MMSE), yielded favorable sample sizes for bvFTD and svPPA, respectively (Table 3). Based on the annual rate of change in CDR box scores a sample size of 71 participants per study arm was calculated for bvFTD, and with annual change in MMSE, a sample size of 86 was calculated for svPPA. The smallest sample size for nfvPPA was 200, based on annual rate of change in CDR box scores.

Overall, annual rate of change in white matter integrity yielded sample sizes below 100 for all disease groups, except bvFTD. For the bvFTD group, annual rate of change in global assessment of functional status yielded the best sample size (Table 4).

Table 3
Sample sizes based on global cognitive and functional scores.

TABLE III. Sample sizes based on global cognitive and functional scores			
Based on cognitive performance			
Groups	CDR_Total	CDR_BoxScore	MMSE
Control	2753	2753	818
bvFTD	172	**71**	143
nfvPPA	521	**200**	251
svPPA	364	114	**86**
AD	385	160	**118**

Illustrated in this table are sample sizes based on annualized rates of change in functional status and cognitive performance. Sample sizes < 100 and highlighted for each pathological group; grey for bvFTD and purple for svPPA.
CDR_Total, total clinical dementia rating score; CDR_BoxScore, box score clinical dementia rating score; bvFTD, behavioral variant frontotemporal dementia; nvfPPA, non-fluent/agrammatic primary progressive aphasia; svPPA, semantic variant primary progressive aphasia, AD, Alzheimer's disease.

Table 4
Summary table of best sample size by group measure of change.

TABLE IV. Summary table of best sample size by group measure of change				
Measure / Group	CDR_BoxScore	MD_SLF L	MD_Fornix	FA_Genu of CC
Control	2753	1790	1999	2269
bvFTD	**71**	581	3879	162
nfvPPA	200	**49**	165	124
svPPA	114	139	**41**	78
AD	160	**23**	1566	1015

Illustrated above a composite table of the change metric with the resultant smallest sample size for at least one group (bvFTD in grey, nfvPPA in yellow, svPPA in purple, and AD in blue, as well as across groups, bordered in red.)
CDR_BoxScore, box score clinical dementia rating score; MD, mean diffusivity; bvFTD, behavioral variant frontotemporal dementia; nvfPPA, non-fluent/agrammatic primary progressive aphasia; svPPA, semantic variant primary progressive aphasia, AD, Alzheimer's disease; FA, fractional anisotropy; MD, mean diffusivity; L, left; SLF, superior longitudinal fasciculus; CC, corpus callosum.

4. Discussion

The present study used DTI to investigate cross-sectional and longitudinal change in the integrity of white matter microstructure in patients with FTD and AD. We sought to evaluate longitudinal DTI metrics (FA and MD) as surrogate biomarkers of disease progression for use in clinical trials. In each clinical variant, we identified regions of white matter where the rate of change was significantly faster in disease groups compared with controls. The patterns generally matched expectations, with changes over time occurring mostly in regions already affected at baseline. FTD groups showed change in anterior more than posterior brain regions, and the AD group mostly in posterior regions. In the PPA and AD groups, tracts were identified where annual rate of change in the white matter microstructure would permit detection of a moderate (40%) reduction in rate of change in a drug trial to be observed with 100 or less subjects per arm. Change rates in white matter in bvFTD gave rise to larger sample sizes; the smallest sample size estimated in bvFTD came from change in global measures of functional status. These findings are generally consistent with prior studies and provide support for DTI as a potential measure of disease progression for clinical trials in FTLD and AD.

When comparing longitudinal white matter degeneration across FTD subtypes we identified some differences across syndromes, but also significant overlap. SvPPA and nfvPPA showed degeneration in tracts that mediate communication with the temporal lobes, including the fornix, uncinate fasciculus, and tapetum. Correspondingly, these tracts are among those that generated the best effect sizes for svPPA and nfvPPA. At the same time, we found that the genu of the corpus callosum showed significant change in these two variants as well as in bvFTD, making it a good candidate region for longitudinal studies that might include more than one FTD subtype. The finding of areas of overlap in white matter degeneration across FTD subtypes is congruent with prior reports of overlap in degeneration of underlying functional networks, and the ensuing symptomatology, in particular between bvFTD and svPPA (Rosen et al., 2002a; Rosen et al., 2002b; Liu et al., 2004). Furthermore, the emergence of the corpus callosum as a tract with a relatively large effect size for change in three separate groups is a highly unlikely finding, and so provides some internal validation that the corpus callosum may indeed prove to be a valuable region for tracking white matter pathology. Interestingly, a recent study of white matter development and degeneration in a large group of healthy subjects ages 5–83 demonstrated that the corpus callosum was one of the first regions to show degeneration due to aging (Lebel et al., 2012).

To date, few studies have investigated longitudinal change in white matter integrity in FTD and AD (Frings et al., 2014; Zhang et al., 2016; Mahoney et al., 2015; Lam et al., 2014; Floeter et al., 2016; Tu et al., 2016), and only one prior study has generated sample size estimates, specifically in bvFTD (Mahoney et al., 2015). Sample size estimates from that study of bvFTD were smaller than the estimates we generated in our bvFTD group. We note that the prior study used a diffusion gradient of 1000 s/mm^2, and acquired two diffusion weighted scans. Both of these approaches might improve signal to noise ratio, contributing to the stability of measurements over time, and therefore generating a smaller sample size estimate. This should be addressed in future studies. Moreover, separate analyses of anatomically distinct groups of bvFTD, such as a slowly progressive, subcortical subtype (Ranasinghe et al., 2016), or genetic bvFTD cohorts may reduce variability and improve sample sizes in this pathologically heterogenous group. It is also notable that, in our analysis, MD generated lower sample size estimates than FA. That said, because this was a relatively small dataset, we did not do a formal analysis of whether MD was a significantly better measure of change in white matter than FA, and we would note that the prior longitudinal study of DTI in bvFTD produced lower sample sizes for FA compared with MD (Mahoney et al., 2015). Thus, any conclusion about which is the better metric for longitudinal tracking would seem premature. FA may have potential advantages over MD because FA is a measure of directionality in white matter tracts rather than absolute diffusion, and therefore increases in diffusion across white matter tracts could be balanced by increases along white matter tracts, which would decrease the magnitude of change detected in FA, without affecting MD. Furthermore, FA and MD reflect many processes that affect microstructural integrity including white matter cellularity and protein deposits, and the extent to which each of these aspects of pathology is involved in a particular form of neurodegeneration could influence the relative sensitivity of FA or MD (Racine et al., 2014). Given the complexity of these processes it is likely premature to make firm conclusions about the contexts in which FA or MD would be the most appropriate measure. Our finding that imaging measures generally allowed for lower sample size estimates than clinical measures is consistent with prior studies in FTLD showing that measures of grey matter volume (Knopman et al., 2009) and white matter integrity (Mahoney et al., 2015) require lower sample sizes than clinical measures. The one exception in this study was bvFTD, where the CDR sum-of-boxes score produced a lower sample size estimate than DTI. The finding that functional measures such as CDR are attractive for clinical trials in FTLD has been highlighted in prior studies (Knopman et al., 2008; Borroni et al., 2010). The fact that this measure was better than imaging specifically in bvFTD can best be interpreted in light of previous findings that the brain regions that change over time are quite heterogeneous across patients with bvFTD, which limits the ability of imaging to improve upon clinical measures (Binney et al., 2017). In contrast, because global measures of function capture the effects from a variety of impairments, they are somewhat immune to the variability in

the specific cognitive and behavioral changes across patients. These observations provide support for methods that would create personalized metrics for disease tracking that are targeted at the clinical or imaging regions most likely to change in that individual, in line with prior proposals of "multiple-n-of-1" designs in clinical trials (Irwig et al., 1995; Tsapas and Matthews, 2008).

It will be important for additional studies to be done on independent, larger cohorts. Such studies will help confirm whether our sample size estimates are reasonable, while ascertaining whether there is consistency regarding the best regions for tracking disease over time. Voxel-wise sample size estimates represent a novel approach to sample size calculation that may produce more sensitive regions of interest tailored to each disease. Future studies could pursue empiric discovery of ideal regions for use as imaging biomarker for therapeutic trials, similar to what has been done for grey matter atrophy (Pankov et al., 2016). In addition, treatments aim to improve functional abilities that clinical measures, such as neuropsychological assessments, aspire to capture. While our data indicate that measures of change in the white matter microstructures could be a valuable surrogate marker of disease state progression, it will be important to verify the relationship between imaging biomarkers and functional and clinical measures before these measures could become acceptable outcomes in treatment studies. Additional work should also be done to define how clinical and imaging data can be best combined to assess both pathological disease state and clinical disease stage progression. Finally, future studies could investigate whether patterns of white matter change can help distinguish underlying molecular pathologies in sporadic as well as familial cases of FTLD at various stages of disease.

In addition to the utility of our findings for clinical trials, with progress in knowledge of molecular and cellular components of FTLD, the need for translational methods of quantifying the various components of pathology *in vivo* increases. Animal models and pathological studies in FTLD have established the importance of persistent microglial activation and the ensuing detrimental effects on white matter integrity. Therefore, the use of white matter imaging for studies of FTLD trajectories has the two-fold advantage of providing a pragmatic, shared measure of therapeutic intervention across clinical subtypes, as well as the potential for specific measurements of therapeutic effects for molecules targeting microglia and white matter degeneration. Last, according to the trans-synaptic hypothesis of spread of neurotoxic proteinopathies, longitudinal patterns of white matter degeneration represent a promising means of tracing the spread of disease.

Author contributions

Fanny Elahi – project conceptualization, statistical analyses and interpretation, manuscript preparation and writing.

Gabe Marx – imaging processing and statistical analyses, manuscript preparation.

Yann Cobigo – imaging processing and statistical analyses, critical revision of manuscript.

Adam Staffaroni – critical revision of manuscript.

John Kornak – statistical advice and critical revision of the manuscript.

Duygu Tosun – critical revision of manuscript.

Adam Boxer – critical revision of manuscript, obtaining funding.

Bruce Miller – critical revision of manuscript, obtaining funding.

Joel Kramer – critical revision of manuscript, obtaining funding.

Howard Rosen – project conceptualization, interpretation of data, critical revision of manuscript, study supervision/coordination, obtaining funding.

Author disclosures

Authors on this manuscript have no disclosures to declare.

Acknowledgments

This project was supported by the National Institutes of Health grant numbers AG045333 and AG045390, AG032306 (H.J.R.), and AG019724 and AG023501 (B.L.M.) and the Hilblom Network Grant 2014-A-004-NET (J.H.K).

Appendix A. Supplementary data

Supplementary data to this article can be found online at http://dx.doi.org/10.1016/j.nicl.2017.09.007.

References

Acosta-Cabronero, J., Patterson, K., Fryer, T.D., et al., 2011. Atrophy, hypometabolism and white matter abnormalities in semantic dementia tell a coherent story. Brain 134, 2025–2035.

Agosta, F., Galantucci, S., Svetel, M., et al., 2014. Clinical, cognitive, and behavioural correlates of white matter damage in progressive supranuclear palsy. J. Neurol. 261, 913–924.

Baborie, A., Griffiths, T.D., Jaros, E., et al., 2011. Pathological correlates of frontotemporal lobar degeneration in the elderly. Acta Neuropathol. 121, 365–371.

Binney, R.J., Pankov, A., Marx, G., et al., 2017. Data-driven regions of interest for longitudinal change in three variants of frontotemporal lobar degeneration. Brain Behav. 7, e00675.

Borroni, B., Brambati, S.M., Agosti, C., et al., 2007. Evidence of white matter changes on diffusion tensor imaging in frontotemporal dementia. Arch. Neurol. 64, 246–251.

Borroni, B., Agosti, C., Premi, E., et al., 2010. The FTLD-modified Clinical Dementia Rating scale is a reliable tool for defining disease severity in frontotemporal lobar degeneration: evidence from a brain SPECT study. Eur. J. Neurol. 17, 703–707.

Boxer, A.L., Geschwind, M.D., Belfor, N., et al., 2006. Patterns of brain atrophy that differentiate corticobasal degeneration syndrome from progressive supranuclear palsy. Arch. Neurol. 63, 81–86.

Brun, A., 1987. Frontal lobe degeneration of non-Alzheimer type. I. Neuropathology. Arch. Gerontol. Geriatr. 6, 193–208.

Floeter, M.K., Bageac, D., Danielian, L.E., Braun, L.E., Traynor, B.J., Kwan, J.Y., 2016. Longitudinal imaging in C9orf72 mutation carriers: relationship to phenotype. NeuroImage 12, 1035–1043.

Frings, L., Yew, B., Flanagan, E., et al., 2014. Longitudinal grey and white matter changes in frontotemporal dementia and Alzheimer's disease. PLoS One 9, e90814.

Galantucci, S., Tartaglia, M.C., Wilson, S.M., et al., 2011. White matter damage in primary progressive aphasias: a diffusion tensor tractography study. Brain 134, 3011–3029.

Garcin, B., Lillo, P., Hornberger, M., et al., 2009. Determinants of survival in behavioral variant frontotemporal dementia. Neurology 73, 1656–1661.

Gorno-Tempini, M.L., Hillis, A.E., Weintraub, S., et al., 2011. Classification of primary progressive aphasia and its variants. Neurology 76, 1006–1014.

Grossman, M., 2010. Primary progressive aphasia: clinicopathological correlations. Nat. Rev. Neurol. 6, 88–97.

Irwig, L., Glasziou, P., March, L., 1995. Ethics of n-of-1 trials. Lancet 345, 469.

Johnson, J.K., Diehl, J., Mendez, M.F., et al., 2005. Frontotemporal lobar degeneration: demographic characteristics of 353 patients. Arch. Neurol. 62, 925–930.

Keihaninejad, S., Zhang, H., Ryan, N.S., et al., 2013. An unbiased longitudinal analysis framework for tracking white matter changes using diffusion tensor imaging with application to Alzheimer's disease. NeuroImage 72, 153–163.

Knopman, D.S., Kramer, J.H., Boeve, B.F., et al., 2008. Development of methodology for conducting clinical trials in frontotemporal lobar degeneration. Brain 131, 2957–2968.

Knopman, D.S., Jack Jr., C.R., Kramer, J.H., et al., 2009. Brain and ventricular volumetric changes in frontotemporal lobar degeneration over 1 year. Neurology 72, 1843–1849.

Lam, B.Y., Halliday, G.M., Irish, M., Hodges, J.R., Piguet, O., 2014. Longitudinal white matter changes in frontotemporal dementia subtypes. Hum. Brain Mapp. 35, 3547–3557.

Lant, S.B., Robinson, A.C., Thompson, J.C., et al., 2014. Patterns of microglial cell activation in frontotemporal lobar degeneration. Neuropathol. Appl. Neurobiol. 40, 686–696.

Lebel, C., Gee, M., Camicioli, R., Wieler, M., Martin, W., Beaulieu, C., 2012. Diffusion tensor imaging of white matter tract evolution over the lifespan. NeuroImage 60, 340–352.

Liu, W., Miller, B.L., Kramer, J.H., et al., 2004. Behavioral disorders in the frontal and temporal variants of frontotemporal dementia. Neurology 62, 742–748.

Mahoney, C.J., Simpson, I.J., Nicholas, J.M., et al., 2015. Longitudinal diffusion tensor imaging in frontotemporal dementia. Ann. Neurol. 77, 33–46.

Mann, D.M., Snowden, J.S., 2017. Frontotemporal lobar degeneration: pathogenesis, pathology and pathways to phenotype. Brain Pathol. http://dx.doi.org/10.1111/bpa.12486. (Jan 18).

Matsuo, K., Mizuno, T., Yamada, K., et al., 2008. Cerebral white matter damage in frontotemporal dementia assessed by diffusion tensor tractography. Neuroradiology 50, 605–611.

Munoz, D.G., Neumann, M., Kusaka, H., et al., 2009. FUS pathology in basophilic

inclusion body disease. Acta Neuropathol. 118, 617–627.
Neumann, M., Sampathu, D.M., Kwong, L.K., et al., 2006. Ubiquitinated TDP-43 in frontotemporal lobar degeneration and amyotrophic lateral sclerosis. Science 314, 130–133.
Pankov, A., Binney, R.J., Staffaroni, A.M., et al., 2016. Data-driven regions of interest for longitudinal change in frontotemporal lobar degeneration. NeuroImage 12, 332–340.
Racine, A.M., Adluru, N., Alexander, A.L., et al., 2014. Associations between white matter microstructure and amyloid burden in preclinical Alzheimer's disease: a multimodal imaging investigation. NeuroImage 4, 604–614.
Ranasinghe, K.G., Rankin, K.P., Pressman, P.S., et al., 2016. Distinct subtypes of behavioral variant frontotemporal dementia based on patterns of network degeneration. JAMA Neurol. 73, 1078–1088.
Rojas, J.C., Boxer, A.L., 2016. Neurodegenerative disease in 2015: targeting tauopathies for therapeutic translation. Nat. Rev. Neurol. 12, 74–76.
Rosen, H.J., Perry, R.J., Murphy, J., et al., 2002a. Emotion comprehension in the temporal variant of frontotemporal dementia. Brain 125, 2286–2295.
Rosen, H.J., Gorno-Tempini, M.L., Goldman, W.P., et al., 2002b. Patterns of brain atrophy in frontotemporal dementia and semantic dementia. Neurology 58, 198–208.
Santillo, A.F., Martensson, J., Lindberg, O., et al., 2013. Diffusion tensor tractography versus volumetric imaging in the diagnosis of behavioral variant frontotemporal dementia. PLoS One 8, e66932.
Schwindt, G.C., Graham, N.L., Rochon, E., et al., 2013. Whole-brain white matter disruption in semantic and nonfluent variants of primary progressive aphasia. Hum. Brain Mapp. 34, 973–984.
Seeley, W.W., 2008. Selective functional, regional, and neuronal vulnerability in frontotemporal dementia. Curr. Opin. Neurol. 21, 701–707.
Smith, S.M., Jenkinson, M., Woolrich, M.W., Beckmann, C.F., Behrens, T.E., Johansen-Berg, H., Bannister, P.R., De Luca, M., Drobnjak, I., Flitney, D.E., Niazy, R.K., Saunders, J., Vickers, J., Zhang, Y., De Stefano, N., Brady, J.M., Matthews, P.M., 2004. Advances in functional and structural MR image analysis and implementation as FSL. NeuroImage 23 (Suppl 1), S208–S219 (PMID: 15501092).
Smith, S.M., Jenkinson, M., Johansen-Berg, H., Rueckert, D., Nichols, T.E., Mackay, C.E., Watkins, K.E., Ciccarelli, O., Cader, M.Z., Matthews, P.M., Behrens, T.E., 2006. Tract-based spatial statistics: voxelwise analysis of multi-subject diffusion data. NeuroImage 31 (4), 1487–1505 (Jul 15, Epub 2006 Apr 19. PMID: 16624579).
Spinelli, E.G., Mandelli, M.L., Miller, Z.A., et al., 2017. Typical and atypical pathology in primary progressive aphasia variants. Ann. Neurol. 81, 430–443.
Tsapas, A., Matthews, D.R., 2008. N of 1 trials in diabetes: making individual therapeutic decisions. Diabetologia 51, 921–925.
Tu, S., Leyton, C.E., Hodges, J.R., Piguet, O., Hornberger, M., 2016. Divergent longitudinal propagation of white matter degradation in logopenic and semantic variants of primary progressive aphasia. J. Alzheimers Dis. 49, 853–861.
Whitwell, J.L., Avula, R., Senjem, M.L., et al., 2010. Gray and white matter water diffusion in the syndromic variants of frontotemporal dementia. Neurology 74, 1279–1287.
Wilson, S.M., Ogar, J.M., Laluz, V., et al., 2009. Automated MRI-based classification of primary progressive aphasia variants. NeuroImage 47, 1558–1567.
Wilson, S.M., Henry, M.L., Besbris, M., et al., 2010. Connected speech production in three variants of primary progressive aphasia. Brain 133, 2069–2088.
Zhang, Y., Schuff, N., Du, A.T., et al., 2009. White matter damage in frontotemporal dementia and Alzheimer's disease measured by diffusion MRI. Brain 132, 2579–2592.
Zhang, Y., Walter, R., Ng, P., et al., 2016. Progression of microstructural degeneration in progressive supranuclear palsy and corticobasal syndrome: a longitudinal diffusion tensor imaging study. PLoS One 11, e0157218.